THE JOURNAL OF PHYSICAL CHEMISTRY A
A JOURNAL OF THE AMERICAN CHEMICAL SOCIETY

pubs.acs.org/JPCA

Article

HF Trimer: A New Full-Dimensional Potential Energy Surface and Rigorous 12D Quantum Calculations of Vibrational States

Jia Li,[#] Patricia Vindel-Zandbergen,[#] Jun Li,[*] Peter M. Felker,[*] and Zlatko Bačić[*]

Cite This: *J. Phys. Chem. A* 2024, 128, 9707−9720

Read Online

ACCESS | Metrics & More | Article Recommendations | Supporting Information

ABSTRACT: HF trimer, as the smallest and the lightest cyclic hydrogen-bonded (HB) cluster, has long been a favorite prototype system for spectroscopic and theoretical investigations of the structure, energetics, spectroscopy, and dynamics of hydrogen-bond networks. Recently, rigorous quantum 12D calculations of the coupled intra- and intermolecular vibrations of this fundamental HB trimer (*J. Chem. Phys.* **2023**, *158*, 234109) were performed, employing an older ab initio-based many-body potential energy surface (PES). While the theoretical results were found to be in reasonably good agreement with the available spectroscopic data, it was also evident that it is highly desirable to develop a more accurate 12D PES of HF trimer. Motivated by this, here we report a new, and the first fully ab initio 12D PES of this paradigmatic system. Approximately 42,540 geometries were sampled and calculated at the level of CCSD(T)-F12a/AVTZ. The permutationally invariant polynomial-neural network based Δ-machine learning approach (*J. Phys. Chem. Lett.* **2022**, *13*, 4729) was employed to perform cost-efficient calculations of the basis-set-superposition error (BSSE) correction. By strategically selecting data points, this approach facilitated the construction of a high-precision PES with BSSE correction, while requiring only a minimal number of BSSE value computations. The fitting error of the final PES is only 0.035 kcal/mol. To assess its performance, the 12D fully coupled quantum calculations of excited intra- and intermolecular vibrational states of HF trimer are carried out using the rigorous methodology developed by us earlier. The results are found to be in a significantly better agreement with the available spectroscopic data than those obtained with the previously existing semiempirical 12D PES.

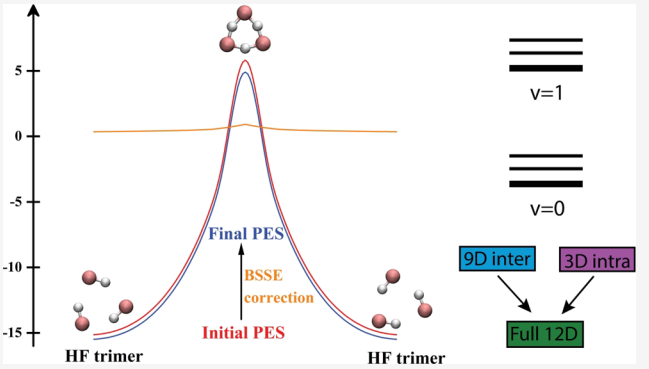

1. INTRODUCTION

Hydrogen bonds are of paramount importance owing to their central role in governing the structural and dynamical properties of liquid and solid phases of water, aqueous solutions, and biomacromolecules such as DNA and proteins. Consequently, over the decades, hydrogen bonding has been intensely investigated by a widening array of ever more sophisticated experimental and theoretical methods. However, high dimensionality and complexity of bulk systems make quantitative characterization of hydrogen bonds, their cooperativity and rearrangement dynamics very difficult, for both spectroscopy and theory.

For this reason, much attention has been focused on smaller hydrogen-bonded (HB) molecular clusters. Their high-resolution infrared (IR), far-IR, and Raman spectra are rich with information pertaining to the multidimensional potential energy surfaces (PESs) of the complexes and their elaborate vibration-rotation-tunneling (VRT) dynamics that often involves multiple potential minima. But, extracting the maximum of this information requires (a) an accurate, ideally full-dimensional PES of the system, covering both its intra- and intermolecular degrees of freedom (DOFs), and (b) the ability to compute rigorously and in full dimensionality the (ro)vibrational eigenstates of the complex using this PES. Only then can a direct and unambiguous comparison be made between the spectroscopic measurements and the theoretical results, allowing for the interpretation and assignment of the former and assessing the quality of the PES employed. For a long time, this approach was feasible only for the binary HB complexes such as HF dimer,[1−5] HCl dimer,[3,6,7] and H_2O dimer.[8]

The scope of binary HB and van der Waals (vdW) complexes amenable to rigorous full-dimensional quantum treatment of their excited intra- and intermolecular (ro)-vibrational states was significantly enlarged by our introduction of a novel computational strategy.[9] It utilizes the eigenstates of

Received: June 5, 2024
Revised: October 22, 2024
Accepted: October 23, 2024
Published: November 1, 2024

reduced-dimension intra- and intermolecular vibrational Hamiltonians, obtained by appropriate partitioning of the full (ro)vibrational Hamiltonian of the molecular complex, as compact contracted bases for both its intra- and intermolecular DOFs, respectively.[9,10] The full Hamiltonian is then diagonalized in the compact final product-contracted basis yielding the desired (ro)vibrational states of the complex.

For a broad range of HB and vdW binary molecular complexes, this approach has enabled for the first time fully coupled quantum calculations in full dimensionality of all intramolecular vibrational fundamentals (and some overtones) and their frequency shifts, as well as the low-energy intermolecular vibrational states in each of the intramolecular vibrational manifolds. This includes water-containing binary molecular complexes for flexible monomers, H_2O/D_2O-CO,[10] HDO-CO,[11] H_2O−HCl,[12] and several of its H/D isotopologues,[13,14] benzene-H_2O/HDO (9D, flexible water and rigid benzene),[15] $H_2O@C_{60}$ (9D, flexible water and rigid C_{60}),[16] and most recently the water dimer (12D).[17] These methodological developments and their applications to binary molecular complexes are reviewed in ref 18 period.

A widely used representation of a PES for an assembly of molecules is by a many-body expansion, as the sum of one-body (monomer), two-body, three-body, and possibly higher-body interactions. Ab initio-calculated 12D 2 + 3-body PESs have been available for a while for two fundamental HB trimers of diatomic molecules, $(HF)_3$ and $(HCl)_3$, described in refs 19−21 respectively. In addition, there was some, although limited, spectroscopic data regarding the fundamental frequencies of certain intra- and intermolecular vibrations for the two trimers, which could be used to test the accuracy of the PESs employed. However, until very recently no methodology existed capable of rigorous full-dimensional (12D) quantum calculations of the intra- and intermolecular vibrational eigenstates of HB trimers of flexible diatomic molecules, the results of which could be compared with the spectroscopic measurements.

This missing link between theory and experiment was finally established when Felker and Bačić, building on the strategy outlined above for noncovalently bound binary molecular complexes,[9,10,18] introduced the computational methodology which for the first time allowed rigorous quantum calculations of the vibrational states of cyclic HB molecular trimers, in this case of diatomic molecules, initially in 9D for rigid monomers,[22] and then in full dimensionality (12D), for flexible monomers.[23] The 12D calculations of the fully coupled excited intra- and intermolecular vibrational states of HB trimers of diatomic molecules employ the full vibrational trimer Hamiltonian, largely derived by Wang and Carrington,[24] that is partitioned into two reduced-dimension Hamiltonians, one in 9D for the intermolecular vibrational DOFs and another in 3D for the intramolecular vibrations of the trimer, and a remainder term. Each of the two Hamiltonians is diagonalized separately and a fraction of their respective 9D and 3D eigenstates is selected for the final compact 12D product contracted basis of both the intra- and intermolecular DOFs, in which the matrix of the full 12D vibrational trimer Hamiltonian is diagonalized.[23]

This methodology was implemented by us in the first 12D fully coupled quantum calculations of monomer-stretch excited intra- and intermolecular vibrational states of the paradigmatic HF trimer[23] and HCl trimer.[25] The calculations encompassed the one- and two-quanta monomer-stretch excited intramolecular vibrational states of both trimers, together with the low-energy intermolecular vibrational states in the intramolecular vibrational manifolds of interest. They revealed significant redshifts of the monomer stretch frequencies in the trimers relative to those of the isolated monomers due to the complexation, as well as manifestations of appreciable coupling between the intra- and intermolecular vibrational modes.

In both cases,[23,25] ab initio calculated 2 + 3-body PESs were employed. For each of the two trimers, this allowed us to investigate the impact that the 3-body terms have on the trimer binding energy and the frequencies of its vibrations. This was achieved by a detailed comparison between the results of the 12D calculations on the 2-body PES, obtained by removing the 3-body term from the original 2 + 3-body PES, and those computed on the 2 + 3-body PES. It demonstrated that the 3-body interactions have a strong effect on the trimer binding energies as well as on their intra- and intermolecular vibrational energy levels.[23,25]

The quantum 12D calculations of HF trimer[23] were performed on the pioneering 2 + 3 body PES by Quack, Stohner, and Suhm, referred to hearafter as QSS, that combines the SO-3 2-body potential[19] with the 3-body term designated HF3BG.[20] The 3-body energies were calculated at the level of the counterpoise-corrected second-order Møller-Plesset perturbation theory (MP2) using a double-ζ Gaussian basis set with polarization functions (DZP + MP2), and fitted by analytical 12D potentials.[20] However, the QSS PES is in fact semiempirical, since its 2-body component was modified empirically to improve the agreement between the calculated energy levels and the experimental results. Spectroscopic data regarding the intra- and intermolecular vibrational frequencies of HF trimers are rather scant. Their comparison with the results of the 12D calculations on the QSS PES showed semiquantitative agreement, demonstrating that there was considerable room for improvement.[23]

This finding has provided the impetus for developing a new and highly accurate, full-dimensional (12D) PES of HF trimer in the present work. The construction of such a PES often involves extensive sampling and calculations,[26] which can be both time-consuming and costly. The "correct and improve" strategy augments the low-level information by integrating the difference between low-level and high-level computations. This process ultimately yields a high-level result. Various methods have been developed based on this idea for constructing PESs, such as the dual-level Shepard interpolation method,[27] the hierarchical construction scheme,[28] and the Δ-machine learning (Δ-ML) method.[29,30] However, these methods lack an efficient and systematic method for sampling when building the difference PES. Liu and Li subsequently introduced a strategy that combines both Δ-ML and permutation invariant polynomial-neural network (PIP-NN), termed as the PIP-NN-based Δ-ML approach.[31] This approach commences with the development of a relatively low-level PES, utilizing a comprehensive data set obtained from low-level calculations. An initial difference PES is constructed by selecting a subset of data points from the existing data set, performing high-level electronic structure calculations on them, and then subtracting the corresponding low-level energies. Leveraging the limited extrapolation capabilities of the Neural Network (NN), the remaining data points, which exhibited significant differences in energies across different PESs, will be selected to finalize the correction PES. This correction PES is then used to augment

https://doi.org/10.1021/acs.jpca.4c03771
J. Phys. Chem. A 2024, 128, 9707−9720

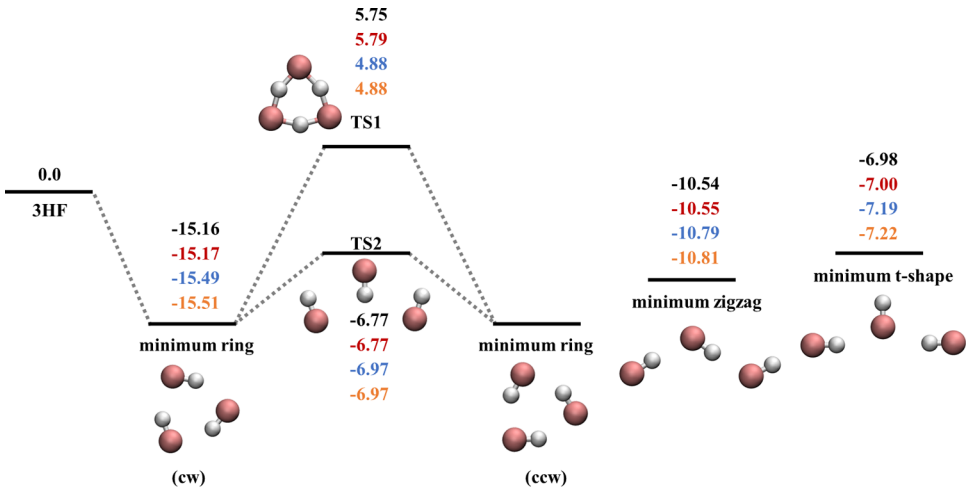

Figure 1. Schematic illustration of the reaction pathways for the HF trimer. From top to bottom, the numbers correspond to PES-2024 (BSSE corrected PIP-NN PES), CCSD(T)-F12a/AVTZ with BSSE, PIP-NN PES without BSSE correction, CCSD(T)-F12a/AVTZ without BSSE. All energies are in kcal/mol and relative to the reactant asymptote 3 HF.

the energies of the remaining data points from low level to high level, resulting in the development of the final high-level PES.

This methodology has been efficaciously implemented in developing the PESs of the multichannel reaction systems HO_2 + HO_2 and CH_3OH + OH.[31,32] Notably, only 14% and 5% of the low-level DFT data sets, comprising 75,300 × 14% and 140,192 × 5% data points, respectively, were required to improve their PESs from the DFT level to the UCCSD(T)-F12a/AVTZ level. Inspired by this methodology, we extended its application to the interaction system CO_2 + N_2, where the difference PES corresponds to the BSSE correction PES.[33] Ultimately, a 97% reduction in the computational cost was achieved for the BSSE correction, thanks to the PIP-NN-based Δ-ML approach.

In this work, the same approach is applied to HF trimer. First, a new full-dimensional PES of HF trimer at the CCSD(T)-F12/AVTZ level is developed. The PIP-NN-based Δ-ML approach helps us to strategically select a subset of points for the development of a BSSE correction PES. The BSSE PES is subsequently utilized for BSSE prediction on the remaining points, culminating in the construction of the final PES that incorporates BSSE correction, denoted hereafter as PES-2024. This completely ab initio PES is employed in 12D fully coupled quantum calculations of excited intra- and intermolecular vibrational states of HF trimer.

Strictly speaking, PES-2024 does not allow rigorous determination of the 3-body interactions, although it is very accurate over rather large intermonomer distances of up to 20 Å covered by our ab initio calculations. Quantifying separate 2- and 3-body interactions requires correct description of the long-range interactions for asymptotic intermonomer distances beyond 20 Å, which PES-2024 does not provide. But, the main goal of this work was to develop a full-dimensional PES capable of yielding highly accurate intra- and intermolecular vibrational levels of HF trimer, for the interpretation and assignment of the existing and future spectroscopic data. The trimer bound states required for this purpose extend over intermonomer distances much smaller than 20 Å. Therefore, their energies are unaffected by the absence of long-range interactions. This is evident from the fact that the agreement of the vibrational states computed in this work on PES-2024 with the spectroscopic data available for HF trimer is markedly better than that for the corresponding results obtained on the (semiempirical) many-body QSS PES[23] (which does include long-range interactions), as shown below. Clearly, the ab initio electronic structure method employed here can and does provide the 12D HF trimer PES whose accuracy in the bound-state region is higher than that of the 12D QSS PES from the 2 + 3-body approach. Unless one is interested in clusters larger than the trimer (which we are not), where having an explicit 3-body term is important, the PIP-NN approach works just as well as the many-body approach when comparison with spectroscopy is desired.

Of course, the above implies that the 2- and 3-body interactions present implicitly (if not explicitly) in PES 2024 are described very accurately within the domain of the PES relevant for spectroscopy. At this time, we have no intention of extending our investigations to HF clusters beyond the trimer. Consequently, quantifying the separate 3-body term has not been our priority. For those interested in larger HF clusters, PES-2024 provides an excellent starting point, and long-range interactions can be added to it in various ways.

The paper is organized as follows. Section 2 describes the new PES, PES-2024, its development, and main features. Section 3 summarizes the methodology for the 12D quantum bound-state calculations. The results for 12D quantum bound states are presented and discussed in Section 3. Section 4 contains the conclusions.

2. 12D POTENTIAL ENERGY SURFACE OF HF TRIMER

2.1. Ab Initio Calculations. In this study, we utilized the MOLPRO 2020.2 software package to perform all ab initio calculations.[34] The CCSD(T)-F12a method, which is an explicitly correlated coupled cluster method with single, double, and perturbative triple excitations, was employed in conjunction with the augmented correlation-consistent valence triple-ζ basis set (CCSD(T)-F12a/AVTZ) to compute the energies, geometries, and harmonic frequencies of all stationary points.[35−38] This approach has proven its efficacy in the construction of PESs for a wide range of systems, both reactive and nonreactive.[12,26,32,39,40] Owing to its faster convergence with respect to the size of the basis set, as compared to the conventional CCSD(T) method, the CCSD(T)-F12 method offers significant numerical advantages. Furthermore, the

https://doi.org/10.1021/acs.jpca.4c03771
J. Phys. Chem. A 2024, 128, 9707−9720

accuracy of CCSD(T)-F12a/AVTZ is comparable to the calculations performed at the CCSD(T)/AV5Z level.[38,41−44]

BSSE arises when investigating interactions among monomers within larger clusters, and is attributable to employing incomplete basis sets for individual subsystems.[45,46] The hierarchical correction scheme proposed by Valiron and Mayer was employed for many-body BSSE calculation[47]:

$$E_{ABC}^{CP} = E_A + E_B + E_C + \epsilon_{AB}^{CP(2)}(AB) + \epsilon_{BC}^{CP(2)}(BC) + \epsilon_{AC}^{CP(2)}(AC) + \epsilon_{ABC}^{CP(3)}(ABC) \quad (1)$$

where the subscripts denote the type of system or subsystem (e.g., monomers A, B, C or dimers AB, AC, BC), while the symbols in parentheses, such as (AB) or (ABC), indicate that the energy is computed using the whole basis set of the entire dimer or trimer. The absence of such notations implies that the energy is calculated in the fragment's own basis set. The $\epsilon_{AB}^{CP(2)} = E_{AB}(AB) - E_A(AB) - E_B(AB)$ represents the interaction energy between subsystems A and B, corrected for BSSE using the standard Boys−Bernardi counterpoise (CP) method,[48] analogously for $\epsilon_{BC}^{CP(2)}$ and $\epsilon_{AC}^{CP(2)}$. The three-body interaction term $\epsilon_{ABC}^{CP(3)}(ABC)$ is expressed as follows:

$$\epsilon_{ABC}^{CP(3)}(ABC) = E_{ABC}(ABC) - E_A(ABC) - E_B(ABC) - E_C(ABC) - \epsilon_{AB}^{CP(2)}(ABC) - \epsilon_{AC}^{CP(2)}(ABC) - \epsilon_{BC}^{CP(2)}(ABC) \quad (2)$$

where $\epsilon_{AB}^{CP(2)}(ABC) = E_{AB}(ABC) - E_A(ABC) - E_B(ABC)$. Analogous expressions apply to $\epsilon_{AC}^{CP(2)}(ABC)$ and $\epsilon_{BC}^{CP(2)}(ABC)$.

2.2. PES Fitting. *2.2.1. PES without BSSE.* The development of PESs is a tripartite process, involving data point sampling, energy calculations, and PES fitting.[26] The initial sampling phase includes comprehensive coverage of the three intramolecular HF stretch coordinates. As depicted in Figure 1, there are two reaction pathways in this system, but only one of them involves bond breaking and formation, with both the reactants and products being minimum-energy cyclic structures. Therefore, in addition to sampling along the reaction path, the majority of data points were sampled in the vicinity of the equilibria. Scans were performed, varying the orientations of three HF molecules, to gather a set of data points. Subsequently, CCSD(T)-F12a/AVTZ calculations were performed to obtain their ab initio energies, thereby facilitating the construction of a primitive PES via fitting. A quasi-classical trajectory (QCT) analysis was conducted on this PES, utilizing a range of initial conditions, to thoroughly explore the configuration space and enrich the data set with new data points. To prevent the addition of data points closely resembling those within the existing data set, we utilized the Euclidean distance $\chi(\{r_i\}, \{r_i'\}) = \sqrt{\sum_i^{15} (r_i - r_i')^2}$ as a geometric criterion for screening the newly introduced points, where χ is defined as the internuclear distances between the new data and existing data.[49] During the screening, we considered the permutation invariance among three identical hydrogen atoms and three identical fluorine atoms (3! × 3!). Comparative analyses were performed to examine the PES by assessing the properties of the stationary points, including energies, geometries, harmonic frequencies, and minimum energy paths. These procedures were iteratively executed to incrementally improve the PES until all relevant dynamical results achieved convergence.

In terms of PES fitting, all the data points were fitted to a PIP-NN functional form.[49−51] The input layer of the NN is composed of low-order PIPs, which are symmetrized monomials derived from Morse-like variables associated with internuclear distances,[52,53]

$$G_n = \hat{S}P_n = \hat{S}\prod_{i<j}^{N} p_{ij}^{l_{ij}} \quad (3)$$

where $p_{ij} = \exp(-r_{ij}/\lambda)$ (λ = 1.5 Å and $i, j = 1-6$), and $\hat{S}$ represents the symmetrization operator that contains all permutation operations.[52,54,55] The feed-forward NN with two hidden layers was employed for fitting,

$$V = b_1^{(3)} + \sum_{k=1}^{K}\left(\omega_{l,k}^{(3)} \times f_2\left(b_k^{(2)} + \sum_{j=1}^{J}\left(\omega_{k,j}^{(2)} \times f_1\left(b_j^{(1)} + \sum_{i=1}^{I}\omega_{j,i}^{(1)} \times G_i\right)\right)\right)\right) \quad (4)$$

Here, I is the number of PIPs within the input layer. The variable $\omega_{j,i}^{(l)}$ represents the weights connecting the ith neuron from the $(l-1)$th layer to the jth neuron in the lth layer, and $b_j^{(l)}$ denotes the biases for the jth neurons in the lth layer. The parameters J and K indicate the number of neurons in the two hidden layers. The hyperbolic tangent function is employed as the nonlinear transfer function for both hidden layers, denoted as f_i (i = 1, 2). The fitting parameters ω and b are optimized using the nonlinear least-squares fitting method to minimize the root-mean-square error (RMSE),

$$\mathrm{RMSE} = \sqrt{\sum_{i=1}^{N_{data}} (E_{output} - E_{target}^{i})^2 / N_{data}} \quad (5)$$

To avoid overfitting, the data set was partitioned into three parts for each NN fitting: the training set (90%), the validation set (5%), and the test set (5%). Various NN architectures with different numbers of neurons in the two hidden layers were tested. For each NN architecture, a total of 100 training iterations were executed. The "early stopping" algorithm was employed to mitigate overfitting.[56] To minimize potential false extrapolation issues arising from edge points in the validation and test sets, only fits exhibiting similar RMSE across all three sets were deemed suitable for the final optimal PES.

2.2.2. BSSE PES. For this system, single-point energy calculations using 2 cores on the Intel Xeon CPU E5−2682 v4 @ 2.50 GHz took 25 min with BSSE correction and 10 min without BSSE correction. Clearly, the need for a large number of single-point energy calculations with BSSE correction for a high-precision PES leads to a significant increase in computational expenses. When computational resources are ample, using the complete basis set (CBS) method is an effective strategy that obviates the need for further BSSE calculations. But in this work, we adopted the recently proposed PIP-NN-based Δ-ML approach to build a correction PES that can predict BSSE on data points without direct BSSE calculations.[31] The details for constructing the correction PES have been elaborated in our previous work on CO_2 and N_2.[33] Briefly, a small subset of data points was selected from the existing data set for the computation of BSSE. Subsequently, we proceeded to fit these data points into an initial BSSE correction PES, and selected four best fits to minimize the

https://doi.org/10.1021/acs.jpca.4c03771
J. Phys. Chem. A 2024, 128, 9707−9720

random errors. Leveraging these four PESs, the BSSE values for the remaining data points were predicted. Due to the limited extrapolation capabilities of NN, the performance may vary in areas that are deficient in data points across different BSSE PESs. The average energy differences D of these data points were calculated by the following formula,

$$D = \frac{\sum_{i,j}^{4} |V_{\mathrm{BSSE}}^{i} - V_{\mathrm{BSSE}}^{j}|}{6} \tag{6}$$

where V_{BSSE}^{i} and V_{BSSE}^{j} denotes the BSSE value obtained by ith and jth BSSE PESs. Then the data points exhibiting significant differences were selected and added to the BSSE data set through a selection process utilizing generalized Euclidean distances.[49] These steps are iteratively performed until convergence is achieved on the PES. In order to evaluate the predictive performance of the BSSE PES, we performed calculations of mean total absolute deviation (MTAD) and root-mean-square deviation (RMSD) for each iteration of PES fitting,

$$\mathrm{MTAD} = \frac{\sum_{i=1}^{N_{\mathrm{data}}} D_i}{N_{\mathrm{data}}} \tag{7}$$

and

$$\mathrm{RMSD} \sqrt{\frac{\sum_{i=1}^{N_{\mathrm{data}}} D_i^2}{N_{\mathrm{data}}}} \tag{8}$$

When the MTAD and RMSD display minimal or insignificant alterations, it signifies the convergence of the model.

2.3. Final PES. Upon the completion of the BSSE PES, predictions of the BSSE values were carried out for the remaining data points. Subsequently, these predicted BSSE values were summed with their corresponding ab initio values without the BSSE correction, resulting in the total energy for each data point, denoted as $E_{\mathrm{total}} = E_{\mathrm{ab\ initio}} + E_{\mathrm{BSSE}}$. In the end, the newly obtained total energies were fitted through the PIP-NN method to obtain the final PES (PES-2024) that includes BSSE correction.

2.4. Diffusion Monte Carlo. The Diffusion Monte Carlo (DMC) is a stochastic approach employed to determine the ground-state energy and vibrational wave function of molecules.[57−59] This is achieved by propagating a group of localized functions, referred to as walkers, through imaginary time, to solve the time-dependent Schrödinger equation,

$$|\Psi(\tau)\rangle = \sum_{n} c_n e_n^{-\tau(E_n - V_{\mathrm{ref}})} |\phi_n\rangle \tag{9}$$

where $|\phi_n\rangle$ is an eigenstate of the Hamiltonian, c_n represents the expansion coefficient, and $\tau = it/\hbar$ is the imaginary time. At each step of imaginary time in the simulation, a random displacement, which follows a Gaussian distribution, is imparted to each walker across every degree. The walker's survival, replication, or removal is determined by a comparison of its potential energy, E_i, with a reference energy, V_{ref},

$$V_{\mathrm{ref}} = \overline{V}(\tau) - \alpha\left(\frac{N_{\mathrm{w}}(\tau) - N_{\mathrm{w}}(0)}{N_{\mathrm{w}}(0)}\right) \tag{10}$$

Here, $\overline{V}(\tau)$ represents the ensemble's average potential energy, and $N_{\mathrm{w}}(\tau)$ denotes the number of walkers at a given imaginary time τ. The second term modifies the value of V_{ref} to maintain a nearly constant ensemble size throughout the simulation, while the parameter α modulates the fluctuations in both the number of walkers and the reference energy. Ultimately, the zero-point energy (ZPE) is estimated as the average of the reference energy over all imaginary times. The statistical uncertainty of the ZPE can be characterized as the standard deviation of the DMC energies, calculated across all of the simulations conducted:

$$\Delta E = \sqrt{\frac{1}{n}\sum_{i=1}^{n} (E_i - \overline{E})^2} \tag{11}$$

where $\overline{E}$ is the average ZPE and n is the number of simulations. All DMC calculations were executed utilizing PyVibDMC, a tool developed by McCoy's group.[60]

2.5. Stationary Points. The reaction pathway for the HF trimer is depicted in Figure 1. Figure S1 presents the optimized geometric parameters of the stationary points, while Table S1 provides a summary of their respective energies and harmonic frequencies. Note that all the energies are relative to the reactant asymptote 3 HF if not specified. As depicted in Figure 1, the global minimum corresponds to the cyclic structure of HF trimer with C_{3h} symmetry, with a depth of −15.2 kcal/mol on the PES-2024. This value aligns well with −15.2 kcal/mol calculated at the level of CCSD(T)-F12a/AVTZ with BSSE correction. Subsequently, the reaction branches in two distinct pathways via saddle points TS1 and TS2, respectively. The minimum energy paths (MEPs) for these two channels are also illustrated in Figure 2. One pathway involves a hydrogen

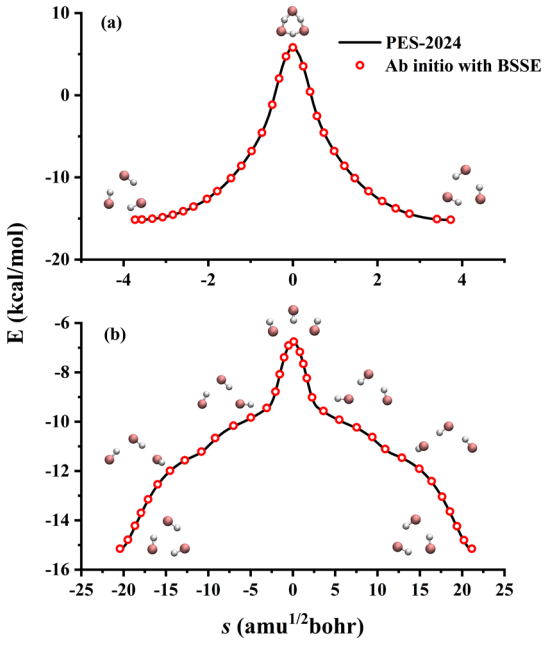

Figure 2. Potential energies along the minimum energy path (MEP) of the (a) R1 and (b) R2 channels on PES-2024 and calculated by ab initio calculations. Energies in kcal/mol are all relative to the reactant asymptote 3 HF.

exchange reaction, characterized by the simultaneous breaking and reforming of all three H-bonds within the cyclic minimum. It corresponds to the interconversion between the clockwise (cw) and counterclockwise (ccw) cyclic arrangements of HF monomers, as depicted in Figures 1 and 2a. In the other pathway, shown in Figure 2b, both the reactants and products also form a minimum ring. However, this pathway diverges

https://doi.org/10.1021/acs.jpca.4c03771
J. Phys. Chem. A 2024, 128, 9707−9720

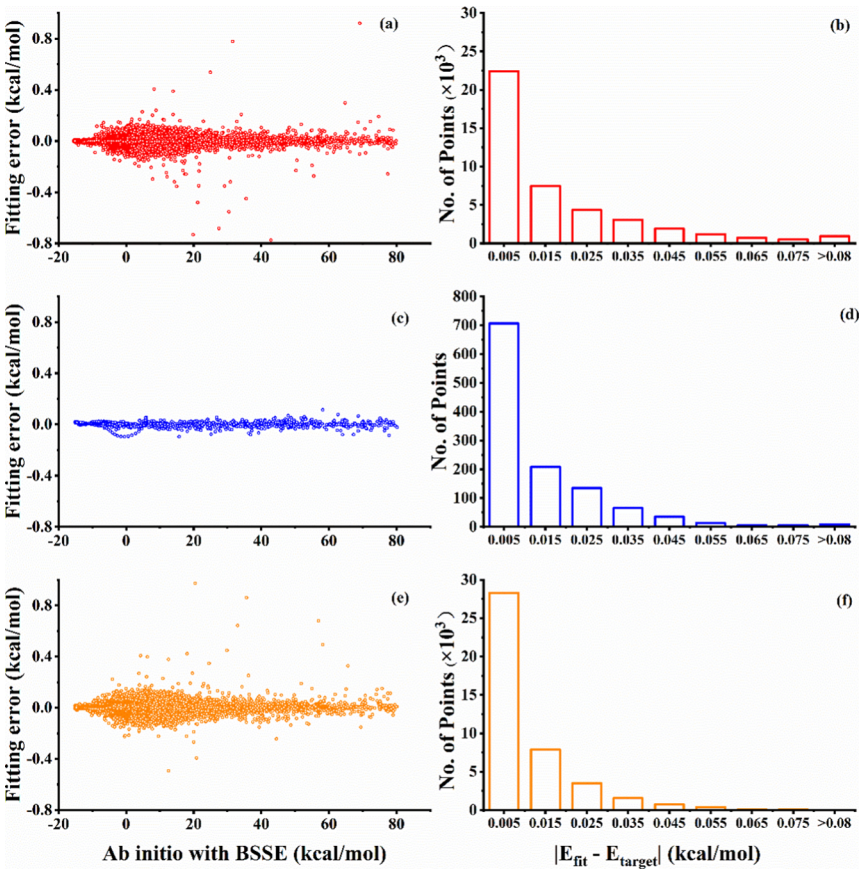

Figure 3. (a,c,e) Fitting errors (defined as $E_{fit} - E_{target}$, in kcal/mol) for the PES without BSSE correction, BSSE correction PES, and PES-2024, respectively, mapped as a function of the target ab initio energy relative to the reactant asymptote. (b,d,f) Distribution analysis of the unsigned fitting errors (defined as $|E_{fit} - E_{target}|$) for the PES without BSSE correction, BSSE correction PES, and PES-2024, respectively.

from the former in the cyclic minimum. It commences with the separation of the three HF molecules. This is followed by a rotation of the hydrogen atom in one HF moiety along the HF bond. Subsequently, an in-plane oscillation involving all three HF molecules leads to the formation of TS2. Ultimately, the structure reverts to the cyclic minimum by retracing the same sequence of events. The two pathways are consistent with the results reported by Quack et al.,[20] where TS1 and TS2 serve as the transition states bridging cw and ccw. However, differing from Quack's results, which characterized the zigzag structure as a saddle point with an imaginary frequency of 70 cm^{-1} and an energy of −6.71 kcal/mol, our PES and ab initio calculations indicate that this structure is a minimum. In addition, HF trimer can form two van der Waals minima, namely the minimum zigzag and t-shape, with energies of −10.5 and −7.0 kcal/mol, respectively. In the work of Orabi et al.,[61] the minima of HF trimer were investigated. They optimized the geometries of the minimum ring and zigzag configurations at the MP2(full)/6-311++G(3df,3pd) level, subsequently calculating their BSSE-corrected energies at the CCSD(T)/6-311++G(3df,3pd) level, which yielded values of −14.0 and −9.7 kcal/mol, respectively. In contrast, the research conducted by Quack et al. reported on the minimum ring and t-shape configurations, obtaining energies of −14.55 and −6.71 kcal/mol, respectively, at the MP2 level with the [8s6p2*d*/6s3p] basis set.[20] Namely, the cyclic HF trimer is more stable than open-chain structures. Based on the analysis of energies, frequencies, and structural parameters, it is evident that for these stationary points the ab initio calculations align well with the results obtained from PES-2024, with the sole exception being the minimum zigzag, which exhibits a slightly imaginary frequency.

2.6. PES Results. As mentioned above, the first step involves constructing a PES without the BSSE correction. The PIP-NN architecture includes an input layer with 738 PIP terms under the maximum order of 5, two hidden layers with 10 and 20 neurons respectively, and a single output for potential energy, amounting to a total of 7631 parameters. This neural network was employed to fit the PES and was trained on approximately 42,540 data points covering the range of intermonomer distances from 1 to 20 Å, which were all calculated at the CCSD(T)-F12a/AVTZ level. The fitting result exhibited RMSEs of 0.026, 0.050, and 0.062 kcal/mol for the training, validation, and testing sets, respectively, with the total RMSE of 0.031 kcal/mol and the maximum deviation of 1.410 kcal/mol. As shown in Figure 3a,b, the fitting errors of this PES are predominantly small and are uniformly distributed across the energy range, which spans from −15.5 to 80 kcal/mol. As seen in Table S1 and Figure S1, the characteristics of the stationary points have been reproduced well on the PIP-NN PES.

The next step is to build a PES that is solely inclusive of BSSE. An initial subset of 284 data points was first selected from the existing 42,540 data set, and were identified along the orientations corresponding to three minima. After several tests, the architecture of the PIP-NN was 227-30-30-1. The remaining points with large D values on the four best PESs according to eq 6 would be added to the BSSE data set after

https://doi.org/10.1021/acs.jpca.4c03771
J. Phys. Chem. A 2024, 128, 9707−9720

screening. This process of adding points is repeated until the MTAD and RMSD values are close and the change is minimal. Figure 4a presents the trend of MTAD and RMSD values with

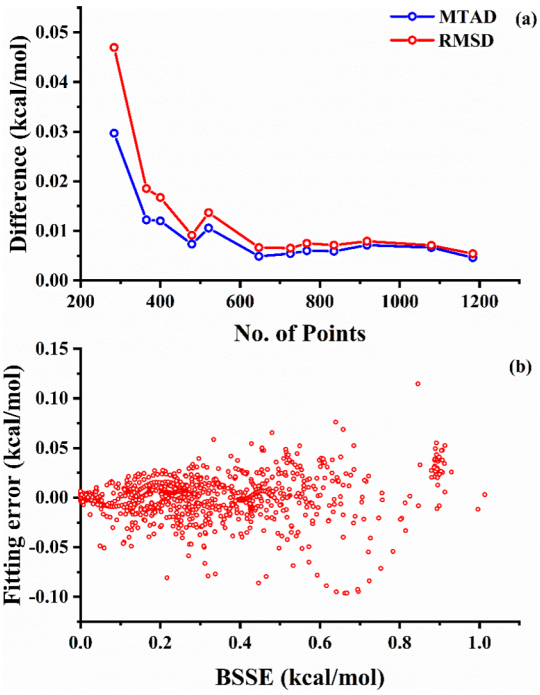

Figure 4. (a) Influence of point counts on MTAD and RMSD dependence for the BSSE correction PES. (b) Fitting errors for the BSSE correction PES as a function of the target ab initio energy.

the increase in the number of the BSSE data points, while Figure 4b displays the distribution of fitting errors on the BSSE PES. Ultimately, a total of 1183 points were selected from 42,540 data points for the construction of the BSSE PES, with the fitting error of 0.021 kcal/mol.

Utilizing the constructed BSSE PES, we predicted the BSSE values for the remaining data points (i.e., 42,540 − 1183 = 41,357). They are combined with the CCSD(T)-F12a/AVTZ energy values to yield the total energies. Next, we gathered the energies of these 41,357 data points, along with the 1183 energies directly derived from ab initio calculations. Using this combined set of data, the PIP-NN method was used to fit the final PES. For the final PES, we utilized a neural network structure of 738-30-30-1, achieving a total RMSE of 0.035 kcal/mol. The RMSEs for the training, validation, and testing sets were 0.055, 0.035, and 0.120 kcal/mol, respectively, with a maximum deviation of 0.159 kcal/mol. Figure 3e,f illustrate the distribution of fitting errors and absolute fitting errors of the final PES. As can be seen from the figure, the fitting errors across the entire energy range are small, with the absolute fitting errors of more than 26,000 data points being less than 0.01 kcal/mol. To more clearly demonstrate the fitting quality across different regions, we have quantified the fitting errors within various energy ranges. For the range of −20 to 0 kcal/mol, there are 22,992 data points with a RMSE of 0.019 kcal/mol; between 0 and 20 kcal/mol, there are 17,319 data points with an RMSE of 0.041 kcal/mol; from 20 to 40 kcal/mol, 1410 data points were recorded with an RMSE of 0.062 kcal/mol; within the 40−60 kcal/mol range, 585 data points were analyzed with an RMSE of 0.074 kcal/mol; and for data points exceeding 60 kcal/mol, there are 232 data points with an RMSE of 0.15 kcal/mol. In addition, in Figure 3c,d we also present the distribution of the fitting errors across the entire total energy range and absolute fitting errors for the BSSE data set. It can be observed that the distribution of points obtained through finite extrapolation sampling using the neural network is similar to the distribution of the total data set, validating the effectiveness of the Δ-ML method. Similarly, Table S1 and Figure S1 collectively provide comprehensive details of the stationary points on the final PES. Figure 2 enhances this further by comparing the PES results for the MEP with the corresponding ab initio calculations. This comparison clearly demonstrates an excellent agreement between the PES and the ab initio results.

Figure 5 presents one-dimensional cuts of the interaction energy between the HF monomers for three different

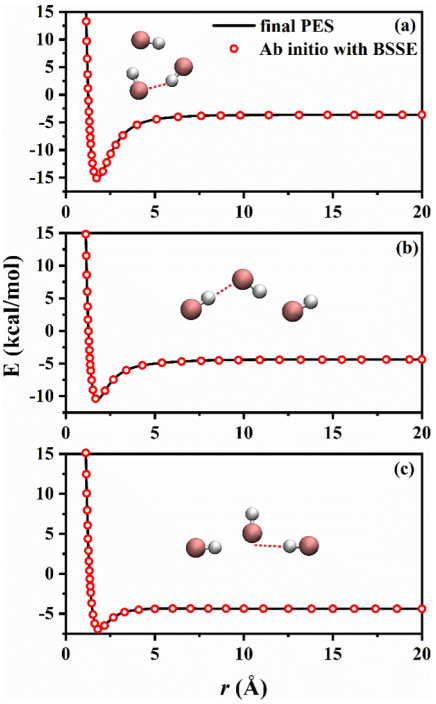

Figure 5. Comparison of one-dimensional cuts for the interaction energy between the three HF monomers at different relative orientations: (a) minimum ring, (b) minimum zigzag, and (c) minimum t-shape. Energies are in kcal/mol relative to the asymptote.

orientations. In Figure 5a, the trimer maintains a cyclic configuration, corresponding to the orientation of the minimum ring, and is then separated as depicted, with a peak deviation of 0.03 kcal/mol between the ab initio and PES results. Figure 5b shows the potentials when the three HF molecules are fixed in the minimum zigzag orientation and then pulled apart in the direction shown in the figure, with a maximum difference of 0.05 kcal/mol. Figure 5c presents the potential energy curve when the trimer is fixed in the T-shape minimum and then distanced along the centroid. The greatest discrepancy is 0.07 kcal/mol. Such minor discrepancies indicate the high precision of the PES in the van der Waals regions. And as seen from these three figures, the energy variation approaches zero as the distance increases. Therefore, a sampling range of 20 Å appears sufficiently large for this system, even for dipole−dipole interactions.

To investigate this system further, we employed the diffusion Monte Carlo (DMC) method to calculate the vibrational zero-

https://doi.org/10.1021/acs.jpca.4c03771
J. Phys. Chem. A 2024, 128, 9707−9720

point energy (ZPE) of the trimer and the ground-state probability amplitude that samples the global minimum on the final PES. In this study, ten independent DMC simulations were carried out. Each DMC trajectory was propagated over 10,000 time steps, with the step size of 5.0 au and 32,000 walkers. The first 20,000 steps were employed to equilibrate the walkers, while the reference energies derived from the subsequent 30,000 steps were utilized to calculate the ZPE. Throughout all simulations, the parameter α was consistently set to 0.1. The final ZPE was calculated by taking the average of the results from ten simulations. This resulted in the value of 7801 cm^{-1} with a standard deviation of 6 cm^{-1} for the minimum ring. For comparison, the harmonic ZPE of the cyclic minimum is 8006 cm^{-1}. Figure 6 presents the

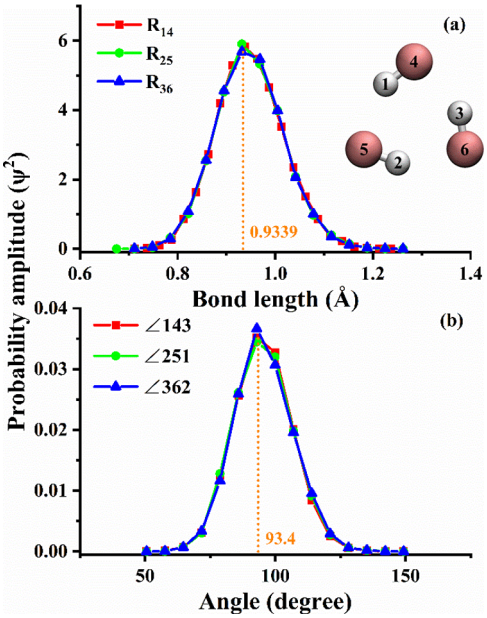

Figure 6. Projection of the DMC probability amplitude onto three H−F bond lengths and HFH angles, with the corresponding equilibrium structure data indicated by the orange dashed line.

projections of the probability amplitude onto the bond length and angle, obtained through the DMC method. As can be observed from Figure 6a, the distribution of bond lengths for the three H−F bonds is essentially consistent, with the maximum value of 0.9317 Å. This is very close to the equilibrium bond length of 0.9339 Å. Similarly, the projection distribution of the three HFH angles in Figure 6b is also remarkably similar, with the maximum value of 92.9°, which is closely aligned with 93.4° found in the equilibrium structure.

3. 12D COUPLED INTRA- AND INTERMOLECULAR VIBRATIONAL STATES OF HF TRIMER

3.1. Computational Methodology. Fully coupled quantum 12D calculations of the intra- and intermolecular vibrational states of HF trimer reported in this paper, that utilize the new PES-2024 presented in Section 2, are performed using the methodology introduced by us for trimers of flexible diatomic molecules.[23] Detailed description of this rigorous 12D approach can be found in ref 23, while the preceding article[22] introduced the 9D rigid-monomer version of this methodology. In both papers,[22,23] the QSS PES[20] of HF trimer was used. Recently, the same methodology was implemented in the 12D fully coupled quantum calculations of the intra- and intermolecular vibrational states of HCl trimer.[25]

Since the methodology for 12D quantum calculations has been described already,[23] here we provide only a brief overview of its salient features, adopting the notation in Section II of ref 23, and focus on discussing the computational details essential for understanding the subsequent sections of this paper.

As in our previous work on cyclic trimers of HB diatomic molecules,[23,25] the trimer coordinates shown in Figure 7,

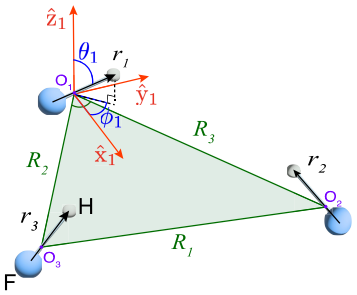

Figure 7. Schematic representation of the coordinates used for the cyclic HF timer with flexible monomers. O_k is the c.m. (center of mass) of each monomer k. Shown explicitly are the three monomer-c.m.-to-monomer-c.m. distances R_k (k = 1−3), and the three intramolecular HF-stretch coordinates, $r_k \equiv |\mathbf{r}_k|$. $\hat{x}_1$, $\hat{y}_1$ and $\hat{z}_1$ are the axes of the local Cartesian system centered at O_1. For monomer k = 1 we also show the azimuthal angle ϕ_1, and the polar angle θ_1 between the HF internuclear vector $\mathbf{r}_1$ and the $\hat{z}_1$ axis. For each monomer k, θ_k and ϕ_k define the orientation of $\mathbf{r}_k$ relative to the local Cartesian axis system attached to monomer k. $\hat{x}_k$ and $\hat{y}_k$ axes are in the $O_1O_2O_3$ plane with $\hat{x}_k$ on the bisector of the angle of the triangle at O_k, and $\hat{z}_k = \hat{x}_k \times \hat{y}_k$, i.e., perpendicular to $O_1O_2O_3$ plane.

introduced by Wang and Carrington,[24] are employed. R_k (k = 1, 2, 3) frame coordinates, collectively denoted as R, refer to the monomer-c.m.-to-monomer-c.m. distances; in effect, they are the intermolecular stretching coordinates of the trimer. The intramolecular HF-stretch coordinates are denoted as r_k (k = 1, 2, 3). The orientation of the kth monomer relative to the local Cartesian axis system attached to that monomer is defined by $\omega_k \equiv (\theta_k, \phi_k)$, k = 1−3, (collectively denoted as ω) where ϕ_k and θ_k are the in-plane and out-of-plane angles, respectively, corresponding to motion in and out of the plane determined by the c.m.-s of the monomers.

The computational methodology outlined in Section 1 relies on the partitioning of the full (12D) vibrational (J = 0) Hamiltonian $\hat{H}$ of the molecular trimer for flexible monomers as follows[23]:

$$\hat{H} = \hat{H}_{\text{inter}}(R, \omega; \bar{r}) + \hat{H}_{\text{intra}}(r; \bar{r}, \bar{\omega}) + \Delta\hat{H}(R, \omega, r; \bar{r}, \bar{\omega}, \bar{r}) \quad (12)$$

.

In eq 12, $\hat{H}_{\text{inter}}(R, \omega;\bar{r})$ is the 9D (rigid-monomer) Hamiltonian for the intermolecular DOFs, $\hat{H}_{\text{intra}}(r;\bar{r}, \bar{\omega})$ is the 3D Hamiltonian for the intramolecular DOFs, and $\Delta\hat{H}(R, \omega, r;\bar{r}, \bar{\omega}, \bar{r})$ is a remainder term; a bar above a symbol denotes a coordinate that is fixed at a suitably chosen value. This partitioning is exact and is done solely for the purpose of generating the contracted inter- and intramolecular bases in 9D and 3D, respectively.

https://doi.org/10.1021/acs.jpca.4c03771
J. Phys. Chem. A 2024, 128, 9707−9720

In order to calculate the 12D eigenstates of $\hat{H}$, we first solve separately for the eigenstates of $\hat{H}_{\text{inter}}$ (a 9D problem) and $\hat{H}_{\text{intra}}$ (a 3D problem) in eq 12. The former yields 9D eigenvectors $|I\rangle$ and corresponding eigenvalues E_I^{inter}, while the latter yields 3D eigenvectors $|\gamma\rangle$ and corresponding eigenvalues E_γ^{intra}. A fraction of these lower-dimensional eigenvectors is used to construct the 12D basis states as products of the form

$$|I, \gamma\rangle \equiv |I\rangle|\gamma\rangle \tag{13}$$

that are symmetrized as outlined in Section 3.2 The matrix of $\hat{H}$ is diagonalized in this 12D symmetrized product-contracted basis. Its matrix elements in the $|I, \gamma\rangle$ basis are given by

$$\langle I', \gamma'|\hat{H}|I, \gamma\rangle = (E_I^{\text{inter}} + E_\gamma^{\text{intra}})\delta_{I',I}\delta_{\gamma',\gamma} + \langle I', \gamma'|\Delta\hat{H}|I, \gamma\rangle \tag{14}$$

Computing the 9D intermolecular eigenstates of $\hat{H}_{\text{inter}}$ is a demanding task in and of itself, that is accomplished by a similar partition-contraction technique.[22] $\hat{H}_{\text{inter}}$ is partitioned into a 3D "frame" Hamiltonian $H_F(R; \bar{\omega}, \bar{r})$ and a 6D "bend" Hamiltonian $\hat{H}_B(\omega; \bar{R}, \bar{r})$, and a remainder term; all three terms are defined in refs 22 and 23. Eigenstates of $\hat{H}_F$ and $\hat{H}_B$ are used to create the 9D product contracted basis, in which $\hat{H}_{\text{inter}}$ is diagonalized.

3.2. Symmetry Considerations. The 12D Hamiltonian $\hat{H}$ of HF trimer in eq 12 is invariant with respect to the operations of the G_{12} molecular symmetry group, which contains the permutations of the monomers and the spatial inversion.[22,23] In order to exploit this symmetry to the maximum, G_{12}-symmetry-adapted basis functions are constructed from the products of the form $|I, \gamma\rangle \equiv |I\rangle|\gamma\rangle$ in eq 13, by the procedure described at length in ref 23. In this symmetrized basis, the matrix of $\hat{H}$ is block-diagonal, with its eight blocks associated with the G_{12} irreps and subirreps.[23] The symmetry blocks are then diagonalized separately, thus greatly reducing the computational effort.

The equilibrium geometry of HF trimer has C_{3h} point-group symmetry. This implies the existence of two equivalent equilibrium geometries, with cw and ccw arrangements of HF monomers, respectively, shown in Figure 1. If the interconversion between the two forms (requiring the concerted breaking and reforming of all three HF-HF hydrogen bonds) is feasible, every vibrational state of the trimer would be split into tunneling doublets, each belonging to one of the following pairs of irreducible representations of G_{12}: (A_1', A_2'), (A_1'', A_2''), (E', E') and (E'', E''). However, the barrier to the cw-ccw conversion is high, 7313.37 cm^{-1} on PES-2024 based on Table 1, and also Figures 1 and 2. Earlier computational studies of HF trimer[22,23,62] have already found negligible splittings (on the order of 10^{-4} cm^{-1}) of the tunneling doublets of the low-energy states. The implication is that cw-ccw tunneling is not feasible at the energies probed by both the calculations and spectroscopy so far, and therefore the effective molecular symmetry group of HF trimer is G_6 (isomorphic with C_{3h}). The same was found for the closely related HCl trimer.[23]

3.3. Convergence Tests. The parameters of the basis sets used in the present 12D calculations on the PES-2024 were carefully tested for convergence, following the procedure described in ref 23. The starting point is provided by the parameters established[23] for the calculations with the QSS PES. However, the implementation of the new PES-2024 requires additional tests in order to refine these basis-set parameters and verify that the 12D calculations using them are converged. These tests involve calculations of the eigenstates of the reduced-dimension Hamiltonians in 3D (inter- and intramolecular), 6D, and 9D, and their results are presented in the Supporting Information.

Table 1. Low-Energy Intermolecular Vibrational States (in cm^{-1}) of HF Trimer from 12D and 9D (Rigid-Monomer) Calculations on PES-2024 in this Work[a]

	PES-2024[b]		QSS PES[c]		assignment
	12D	9D	12D	9D	
A_1', A_2'					
1	0.0	0.0	0.0	0.0	g.s.
2	186.21	189.40	186.90	190.77	ν_{ss}
3	320.11	314.96	328.24	329.51	$2\nu_{as}$
4	368.49	373.42	368.92	376.08	$2\nu_{ss}$
18	764.41	763.55	776.71	775.96	ν_{isb}
E'					
1,2	166.59	163.14	170.91	171.09	ν_{as}
3,4	325.49	319.74	332.73	333.96	$2\nu_{as}$
5,6	347.16	344.53	351.43	353.97	$\nu_{as} + \nu_{ss}$
9,10	493.37	492.35	501.44	498.29	ν_{iab}
A_1'', A_2''					
1	545.89	553.97	556.17	554.98	$\nu_{as} + \nu_{oab}$
2	578.11	584.40	583.98	582.26	$\nu_{as} + \nu_{oab}$
3	600.33	607.56	617.99	614.25	ν_{osb}
4	700.72	708.60	707.98	709.14	
E''					
1,2	412.02	421.88	416.77	414.32	ν_{oab}
3,4	569.38	575.74	576.47	573.27	$\nu_{as} + \nu_{oab}$
5,6	597.69	606.18	599.23	597.69	
7,8	684.24	693.76	699.77	698.27	

[a]Results are compared to the earlier 12D and 9D results on the QSS PES.[23] The 12D results are for the HF monomers in their ground intramolecular vibrational state. [b]12D ground-state energy is −3656.90 cm^{-1} relative to the energy of the separated flexible monomers. The 9D ground-state energy is −3761.27 cm^{-1} relative to the energy of the separated rigid monomers. [c]12D ground-state energy is −3662.35 cm^{-1} relative to the energy of the separated flexible monomers. The 9D ground-state energy is −3812.81 cm^{-1} relative to the energy of the separated rigid monomers.

The final parameters chosen for the computation of the 12D eigenstates of the full vibrational Hamiltonian $\hat{H}$ presented for PES-2024 in this section are the following: the 12D product basis is built from N_{inter} = 600 9D intermolecular eigenstates of $\hat{H}_{\text{inter}}$ with a given parity and N_{intra} = 56 3D intramolecular eigenstates of $\hat{H}_{\text{intra}}$ (encompassing all eigenstates with up to and including five quanta of HF stretch excitations). The 3D intramolecular eigenstates of $\hat{H}_F$ are obtained by its diagonalization in the basis consisting of the products of three 1D potential-optimized discrete variable representation (PODVR)[63,64] functions, with N_r = 8 1D PODVR basis functions per HF-stretch coordinate r_k (k = 1−3); V_{intra} is specified in ref 23. The 6D bend eigenstates of $\hat{H}_B$ are computed in the basis consisting of the products of spherical harmonics $Y_m^l(\theta, \phi)$, and all spherical harmonics with $l \le l_{\max}$ = 13 are included in the final calculations. The 9D intermolecular eigenstates are calculated for $\bar{r} = r_0$ (the rigid-monomer HF bond length, which appears as a parameter in the 6D $\hat{H}_B$ and the 3D $\hat{H}_F$), $\bar{R}$ = 4.976 bohrs (the fixed intermomomer distance that has to be specified for the 6D $\hat{H}_B$), $V_F = V_F^{(\text{avg})}$ (defined in ref 22), N_R = 12 1D PODVR basis functions for each R_k (k = 1, 2, 3) frame (intermonomer) coordinate, N_B = 120 − the total number of 6D bend states of a given parity

https://doi.org/10.1021/acs.jpca.4c03771
J. Phys. Chem. A 2024, 128, 9707−9720

used to build the 9D intermolecular basis, and N_F = 201 − the total number 3D frame states of all symmetries used to build the 9D intermolecular basis. In the above, $\bar{r} = r_0$ is equal to 1.795 bohrs, the expectation value of the HF monomer bond length for the trimer ground state from the quantum 12D calculations on PES-2024, while $\bar{R}$ = 4.976 bohrs is the expectation value of the intermonomer distance $\langle R_k \rangle$ in the ground state of the trimer from the same 12D calculations. As in ref 23, a value of A = 0.1 of the angular grid cutoff parameter was used, which reduced the size of the grid to 7% of the original.

3.4. Results and Discussion. *3.4.1. Intermolecular Vibrational Eigenstates.* Selected low-energy intermolecular vibrational states of HF trimer from full-dimensional 12D quantum calculations on PES-2024, for the monomers in their ground intramolecular vibrational states, and also from the rigid-monomer 9D quantum calculations on the same PES, are presented in Table 1. In addition, for comparison, Table 1 includes the corresponding results of both the 12D and 9D calculations on the QSS PES, taken from Table 5 of ref 23.

From the data reported in Table 1, PES-2024 and QSS PES give very similar 12D binding energies D_0, 3656.90 and 3662.35 cm^{-1}, respectively, which differ by only 5.45 cm^{-1}. We are not aware of any experimental measurement of this quantity that could be compared with our results. We do note that the computed D_0 value is consistent with the DMC-computed trimer ZPE of 7801 ± 6 cm^{-1} (Section 2.6): The D_0 + ZPE = 11,457.9 ± 6 cm^{-1} sum should equal the sum of the energy difference between the PES minimum for the trimer and that for the separated monomers (15.16 kcal/mol = 5302.3 cm^{-1} from Table S1) plus the difference between the ZPE of the separated monomers and the minimum of the PES for the separated monomers (6148.6 cm^{-1}). The latter sum is 11,450.9 cm^{-1}, so agreement between the DMC and variational results is just outside the one-standard-deviation error bar associated with the DMC value.

Inspection of the results in Table 1 for PES-2024 reveals that the 12D and 9D level energies typically differ by 1−4 cm^{-1}, but the differences can occasionally be as large as 8 cm^{-1}. Comparable differences between the 12D and 9D level energies were observed previously for the QSS PES.[23] From this one can conclude that on PES-2024 (and the QSS PES as well[23]) the coupling between the intra- and intermolecular vibrational modes of the trimer is not negligible even when the HF monomers are in their ground state. It has to be included in accurate bound-state calculations and comparisons with experiments, for the purpose of their interpretation and assessing the accuracy of the PES employed.

The assignments of the intermolecular vibrational states on PES-2024 in Table 1 follow those made for the states calculated earlier on the QSS PES.[23] Both sets of states are assigned in terms of the fundamentals, overtones, and combinations of the intermolecular symmetric and asymmetric stretch modes (ν_{ss} and ν_{as}), respectively, as well as the following bending modes: a nondegenerate symmetric mode—ν_{isb} (irrep A_1') and ν_{osb} (irrep A_1''), for the in- and out-of-plane cases, respectively—and two doubly degenerate asymmetric modes—ν_{iab} (irrep E') and ν_{oab} (irrep E'') for the in- and out-of-plane cases, respectively.

Table 1 shows that the 12D intermolecular vibrational states computed on PES-2024 have energies that are lower than those of their counterparts on the QSS PES. The energy differences cover a wide range, as illustrated by the following examples: 0.8 cm^{-1} for ν_{ss}, 4.3 cm^{-1} for ν_{as}, 12.3 cm^{-1} for ν_{isb}, 17.7 cm^{-1} for ν_{osb}. For the other states listed in Table 1, the differences between their energies calculated on PES-2024 and QSS PES fall in the same range. Clearly, PES-2024 and QSS PES have subtle but significant differences concerning their dependence on the intermolecular coordinates of the trimer.

3.4.2. Intramolecular Vibrational Eigenstates and Frequency Shifts. Table 2 gives the energies of the v = 1 HF stretching states ν_{sym}^{HF} and ν_{asym}^{HF} of the HF trimer from 12D calculations in this work on PES-2024, for intermolecular vibrational modes in the ground state. Also shown for comparison are the corresponding results from the 12D calculations on the QSS PES.[23] The frequency of the ν_{asym}^{HF} fundamental calculated on the PES-2024, 3721.76 cm^{-1}, agrees significantly better with the (only) measured gas-phase intramolecular frequency[65] of 3712 cm^{-1}, than that computed on the QSS PES,[23] 3743.05 cm^{-1}.

Table 2. Energies (in cm^{-1}) of the v = 1 HF Stretching States ν_{sym}^{HF} and ν_{asym}^{HF} of HF Trimer from 12D Calculations on PES-2024 in This Work and on the QSS PES from ref 23, for the Intermolecular Modes in the Ground State[a]

PES-2024		QSS PES[23]		assign.
	freq shift		freq shift	
3624.84	−343.45	3679.40	−280.43	ν_{sym}^{HF}
3721.76	−246.53	3743.05	−216.78	ν_{asym}^{HF}

[a]Energies listed are all relative to the relevant ground-state energy. Also shown are their frequency shifts relative to v = 1 vibrational level of the isolated HF, 3968.29 cm^{-1} on PES-2024 and 3959.83 cm^{-1} on the QSS PES.

Complex formation results in the shift the frequencies of the intramolecular vibrations of the constituent monomers away from the vibrational frequencies of the isolated monomers. Such vibrational frequency shifts were characterized accurately in our recent full-dimensional calculations of the inter- and intramolecular vibrational states of binary molecular complexes of H_2O/D_2O−CO,[10] HDO−CO,[11] and HCl−H_2O,[12] as well as the molecular trimers $(HF)_3$ (on the QSS PES)[23] and $(HCl)_3$.[25]

The 12D results in Table 2 allow us to calculate vibrational frequency shifts of the ν_{sym}^{HF} and ν_{asym}^{HF} fundamental of HF trimer for PES-2024. On this PES, for the monomers at large separation, the v = 1 vibrational level of the isolated HF is at 3968.29 cm^{-1}. A glance at the 12D results for PES-2024 in Table 2 shows that the frequencies of the two v = 1 HF stretching states of HF trimer, 3624.84 and 3721.76 cm^{-1}, respectively, are substantially red-shifted in comparison to that of the isolated HF monomer. The calculated frequency shifts (redshifts) of the states ν_{sym}^{HF} and ν_{asym}^{HF} are −343.45 and −246.53 cm^{-1}, respectively. Based on the measured frequencies of the isolated HF-stretch fundamental,[66] 3961 cm^{-1} and that of the asymmetric HF stretch ν_{asym}^{HF} fundamental,[65] 3712 cm^{-1}, the experimental value of the frequency shift of the ν_{asym}^{HF} fundamental of the trimer is −249 cm^{-1}. This is in much better agreement with the corresponding theoretical result on PES-2024, −246.53 cm^{-1}, than the ν_{asym}^{HF} redshift of −216.78 cm^{-1} calculated on the QSS PES.[23]

3.4.3. Effects of HF-Stretch Intramolecular Excitation on the Intermolecular Vibrational States of HF Trimer. One measure of the strength of the coupling between the intramolecular and intermolecular vibrational modes is the

https://doi.org/10.1021/acs.jpca.4c03771
J. Phys. Chem. A 2024, 128, 9707−9720

Table 3. Intermolecular Excitation Energies (in cm^{-1}) in the Ground-State (g.s.) and $v = 1$ ν_{sym}^{HF} and ν_{asym}^{HF} Intramolecular Manifolds of the HF Trimer, from 12D Calculations on PES-2024 in This Work[a]

	PES-2024			QSS PES		
excitation	g.s	ν_{sym}^{HF} [b]	ν_{asym}^{HF} [c]	g.s	ν_{sym}^{HF} [d]	ν_{asym}^{HF} [e]
ν_{as}	166.59	179.29	(178.82,186.16,170.65)[f]	170.91	183.82	(179.28,185.75, 180.76)[f]
ν_{ss}	186.21	198.26	195.94	186.89	198.94	196.35
ν_{iab}	493.37	524.58	(513.63, 524.48, 515.35)	501.43	536.30	(526.67, 534.31, 529.43)
ν_{isb}	764.41	812[g]		776.70	827[g]	
ν_{oab}	412.02	440.37	(428.48, 443.40, 427.67)	416.77	443.29	(433.88, 440.72, 438.05)
ν_{osb}	600.33	636.02	631.07	617.99	651.59	644.57

[a]Also shown for comparison are the corresponding results on the QSS PES from ref 23 (Table VIII). [b]Energies relative to the intramolecular excitation energy of 3624.85 cm^{-1}. [c]Energies relative to the intramolecular excitation energy of 3721.76 cm^{-1}. [d]Energies relative to the intramolecular excitation energy of 3679.40 cm^{-1}. [e]Energies relative to the intramolecular excitation energy of 3743.05 cm^{-1}. [f]Combinations of two *E*-type excitations produce three distinct energy levels. [g]Approximate value due to significant state mixing.

degree to which the intermolecular excitation energies vary across different intramolecular excitation manifolds. In order to quantify this intra/inter coupling in the case of HF trimer, Table 3 lists the energies of the fundamentals of the intermolecular stretching and bending modes of the trimer for both the intramolecular ground state and excited ($v = 1$) ν_{sym}^{HF} and ν_{asym}^{HF} intramolecular vibrational manifolds, from 12D calculations on PES-2024. For comparison, the corresponding results obtained for the QSS PES[23] are given in Table 3 as well. The intermolecular excitation energies shown are obtained by subtracting the energy of the intramolecular vibrational fundamental, ν_{sym}^{HF} or ν_{asym}^{HF}, from the energies of vibrational states involving combined inter- and intramolecular vibrational excitations. A glance at Table 3 reveals that the energies of all intermolecular vibrational modes considered increase appreciably, on both PESs, as a result of the excitation of either HF-stretch fundamental relative to those in the ground intramolecular vibrational state. Thus, on PES-2024, in the HF-excited ν_{sym}^{HF} intramolecular manifold the energies of the intermolecular stretching mode fundamentals ν_{as} and ν_{ss} increase by 12.7 and 12.1 cm^{-1}, respectively, while for the fundamentals of the four intermolecular bending modes the energy increases are larger, ranging from 28.4 cm^{-1} (ν_{oab}) to 35.7 cm^{-1} (ν_{osb}). Exciting the ν_{asym}^{HF} intramolecular vibrational mode results in comparable increases in the energies of the intermolecular vibrational modes considered.

These observations for PES-2024 not only mirror what emerged from the 12D calculations on the QSS PES,[23] but they are in near-quantitative agreement with them, as is readily apparent from the comparison of the corresponding results on the PES-2024 and QSS PES in Table 3. Thus, while the energies of the intermolecular vibrational fundamentals calculated on PES-2024 and QSS PES for the HF monomers in the ground intramolecular vibrational state exhibit non-negligible differences, as pointed out already in Section 3.4.1, the two PESs appear to exhibit remarkably similar coupling between the intra- and intermolecular DOFs of the trimer, at least for the vibrational states considered.

3.4.4. Comparison between Theory and Experiment. There are only limited spectroscopic data regarding the vibrational frequencies of HF trimer. The information available from spectroscopic measurements in the gas phase as well as Ne and Ar matrices is presented in Table 4. There, it is compared to the theoretical results from the 12D calculations on PES-2024 in this work and those computed previously on the QSS PES.[23] It is immediately evident that the fundamental frequencies of the intermolecular vibrational modes ν_{as}, ν_{iab}, and ν_{osb} calculated on PES-2024 in this work agree extremely well, to within 1−2 cm^{-1}, with the corresponding experimental values measured in either the gas phase (ν_{iab} and ν_{osb}) or in Ne matrix (ν_{as}). It is also clear from Table 4 that the fundamentals of the same modes computed on the QSS PES[23] show somewhat worse agreement with the experimental data.

Table 4. Comparison of the Fundamental Vibrational Frequencies (in cm^{-1}) of the HF Trimer from 12D Calculations on the LL and QSS PESs with Spectroscopic Measurements in the Gas Phase and Neon (Ne) and Argon (Ar) Matrices[a]

mode[b]	PES-2024[c]	QSS PES[d]	gas	Ne matrix[67]	Ar matrix[68]
ν_{as} (ν_7)	166.59	170.91		167	152.5
ν_{ss} (ν_3)	186.21	186.90			
ν_{iab} (ν_6)	493.27	501.44	495[69]	477	446
ν_{isb} (ν_2)	764.41	776.71			
ν_{oab} (ν_8)	412.02	416.77			
ν_{osb} (ν_4)	600.33	617.99	602[69]	590	560
ν_{sym}^{HF} (ν_1)	3624.84	3679.40			
ν_{asym}^{HF} (ν_5)	3721.76	3743.05	3712[65]	3706	3702

[a]Calculated frequencies of the intermolecular vibrational modes, shown in the first six rows of the table, are for HF monomers in their ground intramolecular vibrational state. [b]Literature mode notation is given in parentheses. [c]12D calculations in this work. [d]12D calculations from ref 23 (basis IA).

As stated already in Section 3.4.2, concerning the intramolecular vibrational fundamentals, only a single experimental piece of information in the gas phase is available, 3712 cm^{-1}, for the ν_{asym}^{HF} mode.[65] The corresponding 12D value computed on PES-2024, 3721.76 cm^{-1}, agrees with experiment noticeably better than the result obtained for the QSS PES,[23] 3743.05 cm^{-1}. The same holds for the vibrational frequency shift of the ν_{asym}^{HF} fundamental of the trimer, as discussed in Section 3.4.2. This comparison of the theoretical results with the limited spectroscopic data set available leads to the conclusion that the new PES-2024 describes both intra- and intermolecular vibrations of HF trimer with higher accuracy than the QSS PES.

4. CONCLUSIONS

In this paper, we introduce a new full-dimensional PES of HF trimer, referred to as PES-2024, exploiting the advances in ab initio electronic structure theory. This PES involves no empirical adjustments, unlike the semiempirical QSS PES. A data set of 42,540 points calculated at the CCSD(T)-F12a/

https://doi.org/10.1021/acs.jpca.4c03771
J. Phys. Chem. A 2024, 128, 9707−9720

AVTZ level is utilized. To correct for the BSSE, the recently developed Δ-ML method for effective sampling from the entire data set is employed. We then calculate the BSSE values of these points using the hierarchical correction method, which leads to the construction of a BSSE-corrected PES. This correction PES is subsequently used to determine the BSSE values for the remaining data points. Finally, we perform a fit on the total energy, which has been corrected for BSSE, to derive the final PES. The fitting error of the final PES exhibits a minimal fitting error of 0.035 kcal/mol, with a significant reduction of approximately 97% in computational costs.

In order to assess the quality of the new 12D PES-2024 by comparison with the experimental data, and also compare it to that of the older QSS PES,[20] rigorous 12D quantum calculations of the fully coupled intra- and intermolecular vibrational states of HF trimer are performed on it. The computational methodology employed was developed by us recently in ref 23, where it was applied to the 12D calculations of the HF-stretch excited vibrational states of HF trimer on the QSS PES.

The results for PES-2024 show that already for HF monomers in their ground state, the 12D intermolecular level energies typically differ by 1−4 cm^{-1} (and occasionally more) from their counterparts from the rigid-monomer 9D quantum calculations on the same PES. Similar differences between the 12D and 9D level energies were found for the QSS PES.[23] Clearly, the coupling between the intra- and intermolecular vibrational modes of HF trimer cannot be neglected even for the ground state of the monomers when accurate eigenenergies and conclusive comparison with experiments are desired. Moreover, the energies of the 12D intermolecular vibrational states computed on PES-2024 are noticeably lower than those of their counterparts on the QSS PES, indicating subtle differences between the two PESs regarding their dependence on the intermolecular DOFs of the trimer.

This paper also reports for PES-2024 the energies of the ν = 1 HF-stretch excited intramolecular vibrational states of HF trimer from the 12D calculations, together with the intermolecular vibrational states in the excited ν_{sym}^{HF} and ν_{asym}^{HF} intramolecular vibrational manifolds. The frequency of the ν_{asym}^{HF} fundamental calculated on PES-2024, 3721.76 cm^{-1}, is in a significantly better agreement with the (only) measured gas-phase intramolecular frequency[65] of 3712 cm^{-1}, than that computed on the QSS PES,[23] 3743.05 cm^{-1}.

The complexation-induced frequency shifts (redshifts) of the trimer states ν_{sym}^{HF} and ν_{asym}^{HF} calculated in 12D on PES-2024 are −343.45 and −246.53 cm^{-1}, respectively. The latter agrees much better with the experimental value of the frequency shift of the ν_{asym}^{HF} fundamental of the trimer,[65] −249 cm^{-1}, than the corresponding redshift of −216.78 cm^{-1} calculated on the QSS PES.[23]

Based on the 12D calculations for PES-2024, the excitation of either HF-stretch fundamental leads to an appreciable increase of the energies of all intermolecular vibrational modes relative to those in the ground intramolecular vibrational state. Thus, in the HF-stretch excited ν_{sym}^{HF} intramolecular manifold the energies of the two intermolecular stretching mode fundamentals increase by 12−13 cm^{-1}, while for the fundamentals of the four intermolecular bending modes the energy increases are larger, ranging from 28 to 36 cm^{-1}. These results, which reflect the intra/inter mode coupling, agree nearly quantitatively with those from the 12D calculations on the QSS PES, although the energies of the intermolecular vibrational fundamentals calculated on PES-2024 and QSS PES for the HF monomers in the ground intramolecular vibrational state exhibit nonnegligible differences. From this one can conclude that the coupling between the intra- and intermolecular vibrational modes of the trimer on the two PESs appears to be remarkably similar, at least for the vibrational states considered.

A comparison is made between the limited spectroscopic data available regarding the vibrational frequencies of HF trimer in the gas phase and Ne and Ar matrices and the results of the 12D calculations on PES-2024. The calculated fundamental frequencies of the intermolecular vibrational modes ν_{as}, ν_{iab}, and ν_{osb} are in excellent agreement, to within 1−2 cm^{-1}, with the corresponding experimental values measured in either the gas phase (ν_{iab} and ν_{osb}) or in Ne matrix (ν_{as}). The fundamentals of the same modes computed on the QSS PES[23] exhibit somewhat larger differences with the experimental data. It was already noted that the frequency of the ν_{asym}^{HF} fundamental, as well as its frequency shift due to the complex formation, from the 12D calculations on PES-2024, agree with the experimental values significantly better than the corresponding quantities obtained by 12D calculations on the QSS PES. Taking all this into account, one can conclude that the new fully ab initio PES-2024 provides a more accurate description of the intra- and intermolecular vibrations of the HF trimer than the QSS PES. Thus, it represents a benchmark for assessing the accuracy of future PESs for HF trimer.

Our hope is that this study, together with the earlier one in ref 23, will motivate experimentalists to undertake more detailed spectroscopic investigations of HF trimer, which will enable more comprehensive and conclusive comparison with theory and lead to further refinement of the PES of this remarkable trimer.

■ ASSOCIATED CONTENT

Supporting Information

The Supporting Information is available free of charge at https://pubs.acs.org/doi/10.1021/acs.jpca.4c03771.

Convergence tests and additional results for the eigenstates of the intermediate 3D (inter- and intramolecular), 6D, and 9D Hamiltonians (PDF)

■ AUTHOR INFORMATION

Corresponding Authors

Jun Li − *School of Chemistry and Chemical Engineering & Chongqing Key Laboratory of Chemical Theory and Mechanism, Chongqing University, Chongqing 401331, China;* orcid.org/0000-0003-2392-8322; Email: jli15@cqu.edu.cn

Peter M. Felker − *Department of Chemistry and Biochemistry, University of California, Los Angeles, California 90095-1569, United States;* orcid.org/0000-0002-4907-7231; Email: felker@chem.ucla.edu

Zlatko Bačić − *Department of Chemistry, New York University, New York, New York 10003, United States; Simons Center for Computational Physical Chemistry, New York University, New York, New York 10003, United States; NYU-ECNU Center for Computational Chemistry at NYU Shanghai, Shanghai 200062, China;* orcid.org/0000-0003-2033-3147; Email: zlatko.bacic@nyu.edu

https://doi.org/10.1021/acs.jpca.4c03771
J. Phys. Chem. A 2024, 128, 9707−9720

Authors

Jia Li − *School of Chemistry and Chemical Engineering & Chongqing Key Laboratory of Chemical Theory and Mechanism, Chongqing University, Chongqing 401331, China*

Patricia Vindel-Zandbergen − *Department of Chemistry, New York University, New York, New York 10003, United States; Simons Center for Computational Physical Chemistry, New York University, New York, New York 10003, United States;* orcid.org/0000-0003-3719-8199

Complete contact information is available at: https://pubs.acs.org/10.1021/acs.jpca.4c03771

Author Contributions

#Ji.L. and P.V.-Z. contributed equally to this work.

Notes

The authors declare no competing financial interest.

■ ACKNOWLEDGMENTS

Ji.L. and Ju.L. have been financially supported by the National Natural Science Foundation of China (Grant No. 21973009), the Chongqing Talent Program (Grant No. cstc2021ycjh-bgzxm0070), and the Venture and Innovation Support Program for Chongqing Overseas Returnees (Grant No. cx2021071). Prof. Anne B. McCoy and her student Mickey Moonkaen are thanked for their help with the DMC calculations. P.V.-Z, Z.B., and P.M.F. are grateful to the National Science Foundation for its partial support of this research through the Grants CHE-2054616 and CHE-2054604, respectively. P.V.-Z., Z.B., and P.M.F. are also grateful to the Simons Foundation for the computational resources acquired with its support, that were used in this research. P.M.F. is grateful to Prof. Daniel Neuhauser for his support. This work was supported in part through the NYU IT High Performance Computing resources, services, and staff expertise.

■ REFERENCES

(1) Zhang, D. H.; Wu, Q.; Zhang, J. Z. H.; von Dirke, M.; Bačić, Z. Exact full-dimensional bound state calculations for $(HF)_2$, $(DF)_2$, and HFDF. *J. Chem. Phys.* **1995**, *102*, 2315.

(2) Wu, Q.; Zhang, D. H.; Zhang, J. Z. H. 6D quantum calculation of energy levels of HF stretching excited $(HF)_2$. *J. Chem. Phys.* **1995**, *103*, 2548.

(3) Bačić, Z.; Qiu, Y. In *Advances in Molecular Vibrations and Collision Dynamics, Vol. 3*; Bowman, J. M.; Bačić, Z., Eds.; JAI Press Inc.: Stamford, 1998; p 183.

(4) Vissers, G. W. M.; Groenenboom, G. C.; van der Avoird, A. Spectrum and vibrational predissociation of HF dimer. I. Bound and quasibound states. *J. Chem. Phys.* **2003**, *119*, 277.

(5) Huang, J.; Yang, D.; Zhou, Y.; Xie, D. A new full-dimensional *ab initio* intermolecular potential energy surface and vibrational states for $(HF)_2$ and $(DF)_2$. *J. Chem. Phys.* **2019**, *150*, 154302.

(6) Qiu, Y.; Bačić, Z. Exact six-dimensional quantum calculations of the rovibrational levels of $(HCl)_2$. *J. Chem. Phys.* **1997**, *106*, 2158.

(7) Qiu, Y.; Zhang, J. Z. H.; Bačić, Z. Six-dimensional quantum calculations of vibration-rotation-tunneling levels of ν_1 and ν_2 HCl-stretching excited $(HCl)_2$. *J. Chem. Phys.* **1998**, *108*, 4804.

(8) Wang, X. G.; Carrington, T. Using monomer vibrational wavefunctions to compute numerically exact (12D) rovibrational levels of water dimer. *J. Chem. Phys.* **2018**, *148*, 074108.

(9) Felker, P. M.; Bačić, Z. Weakly bound molecular dimers: Intramolecular vibrational fundamentals, overtones, and tunneling splittings from full-dimensional quantum calculations using compact contracted bases of intramolecular and low-energy rigid-monomer intermolecular eigenstates. *J. Chem. Phys.* **2019**, *151*, 024305.

(10) Felker, P. M.; Bačić, Z. H_2O−CO and D_2O−CO complexes: Intra- and intermolecular rovibrational states from full-dimensional and fully coupled quantum calculations. *J. Chem. Phys.* **2020**, *153*, 074107.

(11) Felker, P. M.; Bačić, Z. HDO−CO complex: D-bonded and H-bonded isomers and intra- and intermolecular rovibrational states from full-dimensional and fully coupled quantum calculations. *J. Phys. Chem. A* **2021**, *125*, 980.

(12) Liu, Y.; Li, J.; Felker, P. M.; Bačić, Z. HCl−H_2O dimer: an accurate full-dimensional potential energy surface and fully coupled quantum calculations of intra- and intermolecular vibrational states and frequency shifts. *Phys. Chem. Chem. Phys.* **2021**, *23*, 7101.

(13) Felker, P. M.; Liu, Y.; Li, J.; Bačić, Z. DCl−H_2O, HCl−D_2O, and DCl−D_2O dimers: Inter- and intramolecular vibrational states and frequency shifts from fully coupled quantum calculations on a full-dimensional neural network potential energy surface. *J. Phys. Chem. A* **2021**, *125*, 6437.

(14) Felker, P. M.; Bačić, Z. Inter- and intramolecular rovibrational states of HCl−H_2O and DCl−H_2O dimers from full-dimensional and fully coupled quantum calculations. *Chin. J. Chem. Phys.* **2021**, *34*, 728.

(15) Felker, P. M.; Bačić, Z. Benzene-H_2O and benzene-HDO: Fully coupled nine-dimensional quantum calculations of flexible H_2O/HDO intramolecular vibrational excitations and intermolecular states of the dimers, and their infrared and Raman spectra using compact bases. *J. Chem. Phys.* **2020**, *152*, 124103.

(16) Felker, P. M.; Bačić, Z. Flexible water molecule in C_{60}: Intramolecular vibrational frequencies and translation-rotation eigenstates from fully coupled nine-dimensional quantum calculations with small basis sets. *J. Chem. Phys.* **2020**, *152*, 014108.

(17) Wang, X. G.; Carrington, T. Computing excited OH stretch states of water dimer in 12D using contracted intermolecular and intramolecular basis functions. *J. Chem. Phys.* **2023**, *158*, 084107.

(18) Felker, P. M.; Bačić, Z. Noncovalently bound molecular complexes beyond diatom-diatom systems: full dimensional, fully coupled quantum calculations of rovibrational states. *Phys. Chem. Chem. Phys.* **2022**, *24*, 24655.

(19) Klopper, W.; Quack, M.; Suhm, M. A. HF dimer: Empirically refined analytical potential energy and dipole hypersurfaces from *ab initio* calculations. *J. Chem. Phys.* **1998**, *108*, 10096.

(20) Quack, M.; Stohner, J.; Suhm, M. A. Analytical three-body interaction potentials and hydrogen-bond dynamics of hydrogen fluoride aggregates, $(HF)_n$, $n \geq 3$. *J. Mol. Struct.* **2001**, *599*, 381.

(21) Mancini, J. S.; Bowman, J. M. A new many-body potential energy surface for HCl clusters and its application to anharmonic spectroscopy and vibration-vibration energy transfer in the HCl trimer. *J. Phys. Chem. A* **2014**, *118*, 7367.

(22) Felker, P. M.; Bačić, Z. Intermolecular vibrational states of HF trimer from rigorous nine-dimensional quantum calculations: Strong coupling between intermolecular bending and stretching vibrations and the importance of the three-body interactions. *J. Chem. Phys.* **2022**, *157*, 194103.

(23) Felker, P. M.; Bačić, Z. HF trimer: 12D fully coupled quantum calculations of HF-stretch excited intramolecular and intermolecular vibrational states using contracted bases of intramolecular and intermolecular eigenstates. *J. Chem. Phys.* **2023**, *158*, 234109.

(24) Wang, X. G.; Carrington, T., Jr. An exact kinetic energy operator for $(HF)_3$ in terms of local polar and azimuthal angles. *Can. J. Phys.* **2001**, *79*, 623.

(25) Simkó, I.; Felker, P. M.; Bačić, Z. HCl trimer: HCl-stretch excited intramolecular and intermolecular vibrational states from 12D fully coupled quantum calculations employing contracted intra- and inter-molecular bases. *J. Chem. Phys.* **2024**, *160*, 164304.

(26) Li, J.; Liu, Y. *Machine Learning in Molecular Sciences*; Springer International Publishing: 2023; pp 161−201.

(27) Nguyen, K. A.; Rossi, I.; Truhlar, D. G. A dual-level Shepard interpolation method for generating potential energy surfaces for dynamics calculations. *J. Chem. Phys.* **1995**, *103*, 5522−5530.
(28) Fu, B.; Xu, X.; Zhang, D. H. A hierarchical construction scheme for accurate potential energy surface generation: An application to the F + H_2 reaction. *J. Chem. Phys.* **2008**, *129*, 011103.
(29) Nandi, A.; Qu, C.; Houston, P. L.; Conte, R.; Bowman, J. M. Δ-machine learning for potential energy surfaces: A PIP approach to bring a DFT-based PES to CCSD(T) level of theory. *J. Chem. Phys.* **2021**, *154*, 051102.
(30) Qu, C.; Houston, P. L.; Conte, R.; Nandi, A.; Bowman, J. M. Breaking the coupled cluster barrier for machine-learned potentials of large molecules: the case of 15-atom acetylacetone. *J. Phys. Chem. Lett.* **2021**, *12*, 4902−4909.
(31) Liu, Y.; Li, J. Permutation-invariant-polynomial neural-network-based Δ-machine learning approach: a case for the HO_2 self-reaction and its dynamics study. *J. Phys. Chem. Lett.* **2022**, *13*, 4729−4738.
(32) Song, K.; Li, J. The neural network based -machine learning approach efficiently brings the DFT potential energy surface to the CCSD(T) quality: a case for the OH + CH_3OH reaction. *Phys. Chem. Chem. Phys.* **2023**, *25*, 11192−11204.
(33) Li, J.; Li, J. An accurate full-dimensional interaction potential energy surface of CO_2 + N_2 incorporating Δ-machine learning approach via permutation invariant polynomial-neural network. *Artif. Intell. Chem.* **2023**, *1*, 100019.
(34) Werner, H.-J.; Knowles, P. J.; Knizia, G.; Manby, F. R.; Schütz, M.; Celani, P.; Györffy, W.; Kats, D.; Korona, T.; Lindh, R. *MOLPRO, version 2019.2, a package of ab initio programs*. 2019, https://www.molpro.net.
(35) Dunning, J.; Thom, H. Gaussian basis sets for use in correlated molecular calculations. I. The atoms boron through neon and hydrogen. *J. Chem. Phys.* **1989**, *90*, 1007−1023.
(36) Kendall, R. A.; Dunning, J.; Thom, H.; Harrison, R. J. Electron affinities of the first-row atoms revisited. Systematic basis sets and wave functions. *J. Chem. Phys.* **1992**, *96*, 6796−6806.
(37) Adler, T. B.; Knizia, G.; Werner, H.-J. A simple and efficient CCSD(T)-F12 approximation. *J. Chem. Phys.* **2007**, *127*, 221106.
(38) Knizia, G.; Adler, T. B.; Werner, H.-J. Simplified CCSD(T)-F12 methods: Theory and benchmarks. *J. Chem. Phys.* **2009**, *130*, 054104.
(39) Lu, D.; Chen, J.; Guo, H.; Li, J. Vibrational energy pooling via collisions between asymmetric stretching excited CO_2: a quasi-classical trajectory study on an accurate full-dimensional potential energy surface. *Phys. Chem. Chem. Phys.* **2021**, *23*, 24165−24174.
(40) Qin, J.; Liu, Y.; Li, J. Quantitative dynamics of paradigmatic SN2 reaction OH- + CH3F on accurate full-dimensional potential energy surface. *J. Chem. Phys.* **2022**, *157*, 124301.
(41) Czakó, G.; Szabó, I.; Telekes, H. On the choice of the ab initio level of theory for potential energy surface developments. *J. Phys. Chem. A* **2014**, *118*, 646−654.
(42) Dawes, R.; Ndengué, S. A. Single- and multireference electronic structure calculations for constructing potential energy surfaces. *Int. Rev. Phys. Chem.* **2016**, *35*, 441−478.
(43) Fu, B.; Zhang, D. H. Ab initio potential energy surfaces and quantum dynamics for polyatomic bimolecular reactions. *J. Chem. Theory Comput.* **2018**, *14*, 2289−2303.
(44) Jiang, B.; Li, J.; Guo, H. High-fidelity potential energy surfaces for gas-phase and gas−surface scattering processes from machine learning. *J. Phys. Chem. Lett.* **2020**, *11*, 5120−5131.
(45) Chałasiński, G.; Szcześniak, M. M. State of the art and challenges of the ab initio theory of intermolecular interactions. *Chem. Rev.* **2000**, *100*, 4227−4252.
(46) Skwara, B.; Bartkowiak, W.; Da Silva, D. L. On the basis set superposition error in supermolecular calculations of interaction-induced electric properties: many-body components. *Theor. Chem. Acc.* **2009**, *122*, 127−136.
(47) Valiron, P.; Mayer, I. Hierarchy of counterpoise corrections for N-body clusters: generalization of the Boys-Bernardi scheme. *Chem. Phys. Lett.* **1997**, *275*, 46−55.
(48) Boys, S. F.; Bernardi, F. The calculation of small molecular interactions by the differences of separate total energies. Some procedures with reduced errors. *Mol. Phys.* **1970**, *19*, 553−566.
(49) Jiang, B.; Li, J.; Guo, H. Potential energy surfaces from high fidelity fitting of ab initio points: the permutation invariant polynomial - neural network approach. *Int. Rev. Phys. Chem.* **2016**, *35*, 479−506.
(50) Jiang, B.; Guo, H. Permutation invariant polynomial neural network approach to fitting potential energy surfaces. *J. Chem. Phys.* **2013**, *139*, No. 054112.
(51) Li, J.; Jiang, B.; Guo, H. Permutation invariant polynomial neural network approach to fitting potential energy surfaces. II. Four-atom systems. *J. Chem. Phys.* **2013**, *139*, 204103.
(52) Xie, Z.; Bowman, J. M. Permutationally invariant polynomial basis for molecular energy surface fitting via monomial symmetrization. *J. Chem. Theory Comput.* **2010**, *6*, 26−34.
(53) Bowman, J. M.; Czakó, G.; Fu, B. High-dimensional ab initio potential energy surfaces for reaction dynamics calculations. *Phys. Chem. Chem. Phys.* **2011**, *13*, 8094−8111.
(54) Murrell, J. N.; Sorbie, K. S.; Varandas, A. J. C. Analytical potentials for triatomic molecules from spectroscopic data. *Mol. Phys.* **1976**, *32*, 1359−1372.
(55) Schmelzer, A.; Murrell, J. N. The general analytic expression for S_4-symmetry-invariant potential functions of tetra-atomic homonuclear molecules. *Int. J. Quantum Chem.* **1985**, *28*, 287−295.
(56) Raff, L.; Komanduri, R.; Hagan, M.; Bukkapatnam, S. *Neural Networks in Chemical Reaction Dynamics*; Oxford University Press: 2012; p 106.
(57) Anderson, J. B. A random-walk simulation of the Schrödinger equation: H_3^+. *J. Chem. Phys.* **1975**, *63*, 1499.
(58) Anderson, J. B. Quantum chemistry by random walk. H ^2P, H_3^+, D_{3h}, $^1A_1'$, H_2 $^3\Sigma_u^+$, H_4 $^1\Sigma_g^+$, Be^1S. *J. Chem. Phys.* **1976**, *65*, 4121.
(59) Quack, M.; Suhm, M. A. Potential energy surfaces, quasiadiabatic channels, rovibrational spectra, and intramolecular dynamics of $(HF)_2$ and its isotopomers from quantum Monte Carlo calculations. *J. Chem. Phys.* **1991**, *95*, 28−59.
(60) DiRisio, R. J.; McCoy, A. B. *rjdirisio/pyvibdmc:1.1.8*. 2021 (accessed 2022-12-02).
(61) Orabi, E. A.; Faraldo-Gómez, J. D. New molecular-mechanics model for simulations of hydrogen fluoride in chemistry and biology. *J. Chem. Theory Comput.* **2020**, *16*, 5105−5126.
(62) Wang, X. G.; Carrington, T., Jr. Six-dimensional variational calculation of the bending energy levels of HF trimer and DF trimer. *J. Chem. Phys.* **2001**, *115*, 9781.
(63) Wei, H.; Carrington, T., Jr. The discrete variable representation of a triatomic Hamiltonian in bond length-bond angle coordinates. *J. Chem. Phys.* **1992**, *97*, 3029.
(64) Echave, J.; Clary, D. C. Potential optimized discrete variable representation. *Chem. Phys. Lett.* **1992**, *190*, 225.
(65) Michael, D. W.; Lisy, J. M. Vibrational predissociation spectroscopy of $(HF)_3$. *J. Chem. Phys.* **1986**, *85*, 2528.
(66) Kuipers, G. A.; Smith, D. F.; Nielsen, A. H. Infrared Spectrum of Hydrogen Fluoride. *J. Chem. Phys.* **1956**, *25*, 275.
(67) Andrews, L.; Davis, S. R.; Hunt, R. D. Far infrared spectra of $(HF)_2$ and $(HF)_3$ in solid argon. *Mol. Phys.* **1992**, *77*, 993.
(68) Andrews, L.; Souter, P. F. HF stretching-bending combination bands for small complexes in solid argon. *J. Chem. Phys.* **1999**, *111*, 5995.
(69) Asselin, P.; Soulard, P.; Madebene, B.; Goubet, M.; Huet, T. R.; Georges, R.; Pirali, O.; Roy, P. The cyclic ground state structure of the HF trimer revealed by far infrared jet-cooled Fourier transform spectroscopy. *Phys. Chem. Chem. Phys.* **2014**, *16*, 4797.

https://doi.org/10.1021/acs.jpca.4c03771
J. Phys. Chem. A 2024, 128, 9707−9720